JOURNAL OF COMPUTATIONAL PHYSICS 57, 188–209 (1985)

Sturmian Eigenvalue Equations with a Chebyshev Polynomial Basis

G. DELIC

Department of Physics and Nuclear Physics Research Unit, 1 Jan Smuts Avenue, Johannesburg 2001, South Africa

AND

G. H. RAWITSCHER

Department of Physics, University of Connecticut, Storrs, Connecticut 06268

Received March 22, 1983; revised April 4, 1984

A Chebyshev polynomial basis is proposed for the solution of Sturmian eigenvalue equations of the form $Av = f$ which are encountered in Quantum Scattering theory. A is a non-self-adjoint second order differential operator and the solution is regular at the origin and has an outgoing wave boundary condition asymptotically. Introduction of the boundary conditions of the problem transforms the polynomial expansion into a set of linearly independent basis functions, or Chebyshev set, where each member of the set satisfies the boundary conditions. Substitution of this set into the eigenvalue equation leads to a finite, complex general matrix problem which is solved by conventional techniques. Detailed computation of eigenvalues and eigenfunctions for five cases including analytical and physically realistic examples confirms the inherent polynomial stability of the method characteristic of the minimax norm.

I. INTRODUCTION

Recently a set of basis functions has been proposed [1] for the approximation of integral operators in multichannel two-body quantum scattering theory. This basis, which is discrete, reduces solution of coupled equations in continuous variables to a finite matrix problem. The utility of the basis is dependent on the implementation of an efficient algorithm for the computation of the basis functions and the associated eigenvalues. These are the solutions of a Sturmian eigenvalue problem

$$Av = f \tag{1}$$

where A is a linear second order differential operator which is not self-adjoint

0021-9991/85 $3.00

because it contains a diffuse local interaction potential which is complex. The function f in the problem of interest has the form

$$f = \alpha \bar{V} v \tag{2}$$

where $\bar{V}$ is also a diffuse local complex interaction. Thus, α and v are corresponding eigenvalues and eigenfunctions, which, for the choice of boundary conditions discussed in Appendix A, are complex. However, the spectrum is entirely discrete even though it does not lie on the real axis as is the case for a self-adjoint operator A with a real asymptotic boundary condition for v [2].

Previously [1], the eigenvalue problem of Eq. (1) was solved by a step-by-step, or marching, algorithm and the discrete eigensolutions were ordered according to the number of nodes in the interaction region (Sturmian theory predicts a denumerably infinite number of these). As starting values square well results were used in the marching algorithm. This procedure works well in some cases but fails to find some or all eigenvalues in others. It is this problem which motivated the development of the method discussed in this communication.

In the present approach the solution v of Eq. (1) is approximated in a series of Chebyshev polynomials [3]. Each independent boundary condition gives an equation relating the coefficients of this expansion amongst themselves and this leads to a set of linearly independent approximating polynomials satisfying the boundary conditions. On defining an inner product having the Chebyshev weight, a set of N such functions constitutes the elements of an N-dimensional Hilbert Space and is referred to here as a Chebyshev set. As $N \to \infty$ successive bounds on the eigenvalues of Eqs. (1) and (2) form a convergent sequence because (on the finite interval) the polynomials with complex rational coefficients are dense in the space of functions v [4]. Furthermore, this Chebyshev set enjoys the characteristic property of Chebyshev theory, namely, that out of the class of approximating polynomials, on the interval of approximation, it provides a "best" approximation in the sense that it minimizes the maximum error as $N \to \infty$.

Equation (1) is then solved as a matrix problem where the eigenvectors are the coefficients of the Chebyshev set and the corresponding eigenvalues solve Eq. (1). The method succeeds in all five cases discussed below and displays polynomial convergence for both eigenvalues and eigenfunctions as a function of increasing basis size.

The previous results [1] are duplicated by the present method and extended to physically realistic cases with orbital angular momentum $l \neq 0$ and energies in the range 14 to 987 MeV. Qualitative features of eigenvalues and eigenfunctions are described in detail. It was noted [1] that if A contains an interaction which is a square well and $\bar{V}$ is also a square well, then Eq. (1) may be solved analytically [5]. This is so, even if both interactions are complex, as the eigenvalues are roots of a transcendental equation. This result is useful for checking purposes when developing Chebyshev polynomial methods for diffuse interactions as outlined in Sections II and III. However, the eigenfunctions of such a square well case are spherical

Bessel functions of complex argument which may themselves be used as an expansion basis set for eigensolutions of Eq. (1) with diffuse interactions. Results for this choice of basis set and the method of solution of Eq. (1) for the square well case are reported in a separate communication [6].

The present communication is divided into seven sections and three appendices. Sections II and III introduce the Chebyshev set and the matrix method of solution for the eigenvalue problem. Sections IV to VI detail the five cases to which the method has been applied and results for eigenvalues and eigenfunctions are described. The appendices describe analytical and numerical details of the computations and Section VII summarizes conclusions and points to areas of further study.

II. The Chebyshev Polynomial Basis

Consider the explicit form of Eq. (1)

$$\frac{d^2 v_{lj}(r)}{dr^2} + \left\{k^2 - U_0(r) - \frac{l(l+1)}{r^2}\right\} v_{lj}(r) = \alpha_{lj}\, \bar{U}(r)\, v_{lj}(r) \tag{3}$$

where l refers to orbital angular momentum and takes only integer values, k^2 is a real constant, and

$$k^2 = \frac{2\mu E}{\hbar^2} \tag{4}$$

$$U_0(r) = \frac{2\mu}{\hbar^2} V_0(r) \tag{5}$$

$$\bar{U}(r) = \frac{2\mu}{\hbar^2} \bar{V}(r) \tag{6}$$

with E the center-of-mass energy in million-electron volts of a particle mass μ. The eigenfunctions and eigenvalues carry the subscript lj and are assumed ordered strictly according to increasing magnitude of α_{lj} for fixed l.

The solutions of Eq. (1) required here are regular at the origin and, for all j and fixed l, satisfy an outgoing-wave boundary condition at some radius $r \geq a$ beyond the range of $U_0(r)$ or $\bar{U}(r)$. In the present work $U_0(r)$ and $\bar{U}(r)$ are assumed to decay exponentially in the exterior region and to have no singularities in the interval of approximation. Details of the choice of boundary conditions are given in Appendix A.

Since the regular solution only is required, introduce $u_{lj}(r)$, where

$$v_{lj}(r) = \sqrt{\pi}\left(\frac{r}{2}\right)^{l+1} u_{lj}(r). \tag{7}$$

The function $u_{lj}(r)$ on the interval $r \in [0, a]$ is expanded in a series of shifted Chebyshev polynomials $T_n^*(x^2)$, or $T_{2n}(x)$,

$$u_{lj}(r) = \sum_{n=0}^{\infty} \frac{\varepsilon_n}{2} b_n^{lj}(a)\, T_{2n}(x) \tag{8}$$

and the approximation consists of truncation of the summation at some $n = N$ which is sufficiently large. In Eq. (8), $r = ax$ and ε_n is one when n is zero and two otherwise. The coefficients b_n^{lj} are defined by inversion of (8) and application of the orthogonality property of the Chebyshev polynomials.

In the case that $U_0(r) = \bar{U}(r) = 0$ the coefficients b_n^{lj} are those of the Spherical Bessel function $j_l(kr)$ expanded on the interval $[0, a]$ and may be generated by recurrence [7]. If $U_0(r)$ and $\bar{U}(r)$ are diffuse potentials this is no longer the case. However, an alternative approach is as follows. Substitution of (7) and (8) into (A3) shows that

$$b_0^{lj}(a) = \sum_{n=1}^{N} d_n^l(a)\, b_n^{lj}(a) \tag{9}$$

where

$$d_n^l(a) = -2\left[1 + \frac{4n^2}{l + 1 - aB_l(ka)}\right] \tag{10}$$

and the coefficients b_n^{lj} and constants d_n^l are complex. The second boundary condition at $r = 0$ is satisfied by multiplying all the coefficients b_n^{lj} by an arbitrary constant which is fixed by requiring the normalization given by Eq. (2.4) of [1], namely,

$$\alpha_{lj} \int_0^a dr\, v_{lj}(r)\, \bar{V}(r)\, v_{lj}(r) = 1. \tag{11}$$

Thus, substitution of (9) into (8) shows that the eigenfunctions of (3) may be approximated by a set of linearly independent polynomial functions $t_n^l(x)$, satisfying the boundary conditions of the problem; i.e.,

$$u_{lj}(r) = \sum_{n=1}^{N} b_n^{lj} t_n^l(x) \tag{12}$$

where the summation no longer includes an $n = 0$ term and

$$t_n^l(x) = \frac{d_n^l(a)}{2} T_0(x) + T_{2n}(x). \tag{13}$$

A matrix eigenvalue problem may now be formulated for the coefficients of Eq. (12) and eigenvalues α_{lj} as described in the next section.

III. Matrix Method of Solution

Substitution of the form (7) into the differential equation (3) and multiplication by $r^2 = a^2x^2$ gives

$$A_l u_{lj} = \alpha_{lj} a^2 x^2 \bar{U} u_{lj} \tag{14}$$

where the operator A_l is defined as

$$A_l = x^2 \frac{d^2}{dx^2} + 2(l+1)\, x \frac{d}{dx} + a^2x^2k^2 - a^2x^2U_0(ax). \tag{15}$$

Using properties of Chebyshev polynomials [8, 9] it follows that

$$A_l t_n^l(x) = C_n^l(x) + D_n^l(x) \tag{16}$$

where the functions C and D are defined as

$$C_n^l(x) = \sum_{k=0}^{n} \frac{\varepsilon_k}{2} \frac{\varepsilon_{n-k}}{2} 4n(2n^2 - 2k^2 + 2l + 1)\, T_{2k}(x) + 4n^2 T_{2n}(x), \tag{17}$$

with

$$D_n^l(x) = a^2x^2k^2 t_n^l(x) - a^2x^2U_0(ax)\, t_n^l(x) \tag{18}$$

and by definition

$$\bar{D}_n^l(x) = a^2x^2\bar{U}(ax)\, t_n^l(x). \tag{19}$$

Substitution of Eq. (12) into (14), multiplication by each of the functions

$$t_{n'}^l(x), \qquad n' = 1,..., N, \tag{20}$$

and integration over x with respect to the weight function $1/\sqrt{1-x^2}$ leads to the $N \times N$ complex general matrix eigenvalue problem

$$\mathbf{R}\mathbf{b}^l = \alpha_l \mathbf{H}\mathbf{b}^l. \tag{21}$$

There are N eigenvectors $\mathbf{b}^l$, of coefficients b_n^{lj}, $n = 1,..., N$, corresponding to N eigenvalues α_{lj}, $j = 1,..., N$.

Defining the scalar product

$$(h, f) = \int_{-1}^{+1} h(x)\, f(x) \frac{dx}{\sqrt{1-x^2}} \tag{22}$$

then the matrix elements of $\mathbf{R}$ and $\mathbf{H}$ are

$$R_{n'n} = (t_{n'}^l, C_n^l) + (t_{n'}^l, D_n^l) \tag{23}$$

and

$$H_{n'n} = (t^l_{n'}, \bar{D}^l_n). \tag{24}$$

Using Eqs. (13) and (17) with the orthogonality property of the Chebyshev polynomials it follows that

$$(t^l_{n'}, C^l_n) = 2n\{c^l_{n0} d^l_{n'} + \varepsilon_{n-n'} c^l_{nn'} + 2n\,\delta_{nn'}\}\frac{\pi}{2} \tag{25}$$

where

$$c^l_{nn'} = 0, \qquad n' > n$$

and $\delta_{nn'}$ is the Kronecker delta function. Assuming the Chebyshev expansions

$$D^l_n(x) = \sum_{m=0}^{N} \frac{\varepsilon_m}{2} h^n_m T_{2m}(x), \tag{26a}$$

$$\bar{D}^l_n(x) = \sum_{\bar{m}=0}^{N} \frac{\varepsilon_{\bar{m}}}{2} \bar{h}^n_{\bar{m}} T_{2\bar{m}}(x) \tag{26b}$$

then

$$(t^l_{n'}, D^l_n) = \left\{\frac{d_{n'}}{2} h^n_0 + h^n_{n'}\right\}\frac{\pi}{2}, \tag{27a}$$

$$(t^l_{n'}, \bar{D}^l_n) = \left\{\frac{d_{n'}}{2} \bar{h}^n_0 + \bar{h}^n_{n'}\right\}\frac{\pi}{2}, \tag{27b}$$

and h^n_m, $\bar{h}^n_{\bar{m}}$ are simply related to the Chebyshev expansion coefficients of $U_0(r)$ and $\bar{U}(r)$ as shown in Appendix B.

The matrix **R** is not symmetric because of the first term in (23). However, the second term is symmetric as is the matrix **H**. Both matrices are complex and neither is Hermitian; however, assume the decomposition

$$\mathbf{H} = \mathbf{W}\Lambda^{1/2}(\mathbf{W}\Lambda^{1/2})^{\mathrm{T}}, \tag{28}$$

where T denotes transpose and **W** is the matrix of eigenvectors of **H** with Λ the diagonal matrix of corresponding eigenvalues. The complex general eigenvalue problem of Eq. (21) is then solved as follows.

ALGORITHM R

(1) Form **H** as in Eq. (24).

(2) Solve $\mathbf{H}\mathbf{y} = \lambda\mathbf{y}$.

(3) Form $\mathbf{K} = \mathbf{W}\Lambda^{-1/2}$.

(4) Form **R** as in Eq. (23).

(5) Form $\mathring{\mathbf{R}} = \mathbf{K}^{\mathrm{T}}\mathbf{R}\mathbf{K}$.

(6) Solve $\mathring{\mathbf{R}}\mathring{\mathbf{b}} = \alpha\mathring{\mathbf{b}}$.

(7) Form $\mathbf{b} = \mathbf{K}\mathring{\mathbf{b}}$.

In step (3) $\mathbf{W}$ contains eigenvectors $\mathbf{y}$ normalized such that $\mathbf{W}\mathbf{W}^{\mathrm{T}} = \mathbf{1}$. The eigenvectors $\mathring{\mathbf{b}}$ in step (6) of Algorithm R (and consequently $\mathbf{b}$) are, in general, not normalized after diagonalization. If only eigenvalues are required then step (7) and normalization are omitted. However, for the results discussed in Section VI the eigenvectors are normalized as follows. Substitution of Eq. (7) into Eq. (11) gives

$$\pi a \left(\frac{a}{2}\right)^{2l+2} \alpha_{lj} \int_0^1 dx\, x^{2l+2} u_{lj} \bar{V} u_{lj} = 1. \tag{29}$$

The numerical evaluation of the integral is described in Appendix C.

If the unnormalized eigenvector $\mathbf{b}^{(u)}$ is used then the result of Eq. (29) is not 1 but $\xi_{lj}^2 \neq 1$, and normalized eigenvectors $\mathbf{b}$ are obtained from $\mathbf{b}^{(u)}/\xi$. However, this procedure does not determine the overall sign of $\mathbf{b}$, nor does matching the logarithmic derivative of Eq. (A3). Furthermore, corresponding eigenvectors of matrices of different order N, $N+2$, etc., can differ in an overall sign.

This phase factor is fixed by requiring, as in (A2), that at $r = a$ $v_{lj}(a) = H_l(ka)$. The v_{lj} so defined are those discussed in Section VI and they differ in normalization (Eq. (2.5) of Ref. [1]) from those defined by (11) although the same notation v_{lj} is used here.

IV. Five Case Studies

To illustrate the application of Algorithm R and study the convergence properties of the method proposed in Sections II and III five examples were chosen and are referred to as cases one to five. In all cases $V_0(r)$ was taken equal to $\bar{V}(r)$ and Table I lists the potential parameters of $\bar{V}(r)$ as well as the truncation radius used in each case. Case two is the Soper potential discussed in [1] and cases three and four are Woods–Saxon potentials approaching the square well of case one which were also discussed in [1] (cf. Fig. 2 of that reference). In the previous work eigenvalues and eigenfunctions for cases two to four were computed using the Numerov marching algorithm for $l = 0$, $k = 0.79722$ fm^{-1}, $2\mu/\hbar^2 = 0.045018$ fm^{-2} MeV^{-1}, and $R = 3$ fm. Here these results of the Numerov method where repeated and extended to case five for $l = 0$ to 14.

Convergence of Algorithm R has been studied as a function of

(A) $N_v + 1$, the number of Chebyshev coefficients in the expansion of V_0 and $\bar{V}$ in Eqs. (B1) and (B2),

(B) a, the truncation radius in r, and

(C) N, the order of the matrix in Eq. (21).

TABLE I

Potential Parameters of $\bar{V}(r)$ for Cases One to Five

Case[a]	Real part		Imaginary part		Truncation radius
	$\bar{V}_0$ (MeV)	$d_{\bar{v}}$ (fm)	$\bar{W}_0$ (MeV)	$d_{\bar{w}}$ (fm)	a (fm)
One	−50	—	0	—	3
Two	−50	0.5	0	—	7.39
Three	−50	0.2	0	—	4.75
Four	−50	0.08	0	—	3.70
Five	−25	0.5	−5	0.5	7.39

[a] With a radius of $R = 3$ fm in all cases, the radial form of the potentials was, for case one, Real $\bar{V}(r) = \bar{V}_0$, $r \in [0, R]$; for cases two to five, Real $\bar{V}(r) = \bar{V}_0/\{1 + \exp[(r-R)/d_{\bar{v}}]\}$; for case five, Imaginary $\bar{V}(r) = 4\bar{W}_0 \exp[(r-R)/d_{\bar{w}}]/\{1 + \exp[(r-R)/d_{\bar{w}}]\}^2$.

Convergence as a function of N has also been studied for increments in energy E from 14.11 to 987 MeV for $l = 0$ for all five cases of Table I. For the lowest energy marching and matrix algorithms are compared in detail for $l = 0$, 4, and 6 in case five.

This section is concluded with some details on the only non-trivial numerical operations involved in Algorithm R. These are computation of the coefficients $\bar{g}_{\bar{p}}$, g_p of Eqs. (B3) and (B4), Coulomb functions $H_l(ka)$ and derivatives $H_l'(ka)$ of Eqs. (A2) and (A3), and numerical matrix solution of Algorithm R.

The only integrals of the matrix method which need to be evaluated numerically are those of Eqs. (B3) and (B4). Since there are some 100 of these at the most, sufficient accuracy is obtained at negligible cost in computing time with a seven point Newton–Cotes quadrature [10] with a step size of 0.005 fm. In the last subinterval, to avoid the singularity at $x^2 = 1$, a formula which does not require the end points is applied.

All the calculations reported here refer to cases where $V_0(r)$ does not contain a Coulomb term. Thus the Sommerfeld parameter η is zero and F_l, G_l, Eq. (A2), were computed with the subroutines of [11] using a value of $\eta = 10^{-6}$ to 10^{-7}. Variation of η in this range produced only changes of the order of one digit in the fourth figure of the largest eigenvalues of cases two to five.

The matrix diagonalizations of Algorithm R were performed by using the CBAL, COMHES, COMLR2, and CBAK2 subroutines of the Matrix Eigensystem Routines EISPACK [12]. This procedure determines all eigenvalues and eigenvectors of a complex $N \times N$ matrix. Excluding time taken for computation of $\bar{g}_{\bar{p}}$, g_p, H_l, H_l', and normalization of eigenvectors, Eq. (29), typical performance for Algorithm R is t (sec) $= 2.36 \times 10^{0.049(N-20)} \sim 2.4$ to 69 s with $N = 20$ to 50 on an IBM 3083E8 processor with double precision arithmetic.

V. Convergence for Eigenvalues

In this and the following section the numerical behaviour of the method is analysed for the five cases of Table I with a view to displaying its inherent numerical stability. Cases one to four of Table I are of interest more from the point of view of verifying coding and substantiating the method while case five is an example of a relatively "difficult" but also physically realistic potential. Therefore, results of case five are discussed in more detail and Section VI shows results only for this case.

Analysis of convergence to a prescribed accuracy must provide answers to the points raised in Section IV. How many polynomials are required to approximate $V_0(r)$ and $\bar{V}(r)$ and what is the best choice of truncation radius? What is the required order N of the matrix for a prescribed accuracy? How is convergence affected by changes in E or l in Eq. (3)? The prescribed accuracy of eigenvalues computed by Algorithm R (unless otherwise stated), is convergence to within one digit in the fourth significant figure for both real and imaginary parts.

Comparison between results of the marching algorithm (Table I of [1]) and the matrix method for $l=0$, $E=14.11$ MeV with $N_v=24$ and $a=7.39$ fm showed that agreement is generally satisfactory but a more detailed comparison is limited by truncation error of the Numerov marching algorithm. For this reason the square well of case one has been included and results for $l=0$ computed from the analytical formulae as described in [6] for $kR=2.392$ to 19.13. The comparison with these analytical results is important as it should show if the R algorithm converges to the exact result.

A. *Convergence as a Function of* N_v ($E=14.11$ *MeV*, $l=0$)

With the truncation radius $r=a$ fixed at some point where $\bar{V}(r)$ $(=V_0(r))$ is $\sim 5\times 10^{-3}$ MeV, then, for a given value of N_v in (B1) and (B2), the R algorithm of order N produces N eigenvalues. These eigenvalues converge, as a function of N, if N is incremented until the prescribed error is reached (see (C) below). If N_v is incremented and the polynomial approximation of the potentials improved then the eigenvalues produced by the R algorithm again converge as a function of N. However, in this case the eigenvalues will be closer to the exact values.

Table II summarizes results for cases two to four giving N_v and indicating with an asterisk where convergence (as a function of N_v) has not reached the prescribed accuracy. In Table II, for each j, first, second, third, and fourth lines correspond respectively to cases two, three, four, and one, i.e., decreasing diffuseness $d_{\bar{v}}$. N is the order of the matrix which produced convergence (as a function of N) to within the prescribed error. The entry SQ, for each eigenvalue, is the result of algorithm R applied to the square well which cases two to four approach. The entry SQ is identical to the analytical result obtained from the method of [6]. Thus, the R algorithm gives the exact eigenvalues of the square well and also the previously observed behaviour [1] of the spectrum as $\bar{V}$ approaches the square well.

TABLE II

Convergence to the Square Well[a-c]

j	N_v	N	Real	Imaginary	Magnitude
1	10	16	−0.09983	−0.2350	0.2553
	8	12	−0.06343	−0.2040	0.2137
	12	14	−0.05621	−0.1971	0.2050
	SQ	4	−0.05471	−0.1957	0.2032
2	14	20	0.6525	−0.4737	0.8063
	10	14	0.8059	−0.3142	0.8650
	10	14	0.8311	−0.2654	0.8725
	SQ	6	0.8338	−0.2542	0.8717
3	18	22	2.103	−0.7104	2.220
	16	20	2.623	−0.3949	2.653
	12	16	2.753	−0.2746	2.767
	SQ	8	2.768	−0.2434	2.779
4	20	28	4.198	−0.9628	4.307
	18	22	5.284	−0.5032	5.308
	18	20	5.636	−0.2989	5.644
	SQ	10	5.688	−0.2398	5.693
5	18	26	6.933	−1.220	7.039
	20	24	8.763*	−0.6249*	8.786*
	20	22	9.457*	−0.3325*	9.463*
	SQ	12	9.585	−0.2384	9.588
6	18	30	10.31	−1.477	10.41
	20	26	13.05	−0.7501*	13.08*
	20	28	14.20	−0.3723*	14.20*
	SQ	14	14.46	−0.2376	14.46
7	18	32	14.33	−1.738	14.43
	20	28	18.16	−0.8778*	18.18*
	20	30	19.88	−0.4187*	19.88
	SQ	16	20.30	−0.2372	20.30
8	18	38	18.99	−1.999	19.10
	16	26	24.10	−1.008	24.12
	20	32	26.44	−0.4712*	26.44
	SQ	16	27.12	−0.2370	27.12
9	18	40	24.29	−2.265	24.40
	20	32	30.82	−1.138*	30.84*
	20	36	33.91	−0.5204*	33.91
	SQ	18	34.92	−0.2367	34.92

[a] $E = 14.11$ MeV and $l = 0$.

[b] The SQ entry for each j is the R algorithm result for a matrix of order N giving convergence of one digit in the fourth figure.

[c] The asterisk indicates those numbers where the convergence as a function of N_v is not yet one digit in the fourth figure but is at most ten times larger.

Also, in view of the results of Table II, a value $N_{\bar{v}} = 24$ was considered as sufficient for all subsequent calculations.

B. *Convergence as a Function of a* ($E = 14.11$ *MeV*, $l = 0$)

The truncation radius should be chosen as small as possible, but still in the region where $\bar{V}(r)$ is negligible. The truncation radii used in the present calculations are given in Table I. A study of case two showed that smaller eigenvalues are less sensitive to truncation radius variations than larger ones. Similar results hold for case five where variation of the $j = 1$ to 9 eigenvalues for $a = 4.93$ to 7.39 fm was studied. The latter values when compared to the marching algorithm results for $l = 0$ show that to produce accuracy of the order of three significant figures for eigenvalues of magnitude up to ~ 57 the truncation radius a should be chosen in the region where neither real nor imaginary parts of $\bar{V}$ are larger than ~ 0.1 percent of their maximal values.

C. *Convergence as a Function of Matrix Order N* ($E = 14.11$ *MeV*, $l = 0$)

Once N_v and a are fixed the convergence of each eigenvalue to the prescribed error limit may be studied as a function of matrix order N. Figure 1 shows the rate of convergence to a prescribed error of one digit in the Sth significant figure as a function of N for the square well. This shows that to obtain three significant figures for eigenvalue $j = J$ a matrix of order $N = 2J$ should be diagonalized [13] and for each additional significant figure the matrix order is incremented by one. This comparison with the analytical result of the square well demonstrates the rapidly improving bound on the eigenvalue computed in the R algorithm. Figure 2 shows the effect of increasing diffuseness $d_{\bar{v}}$ (cases four, three, and two) and the more realistic example of case five. In general the *rate* (i.e., slope) of convergence of all eigenvalues is largely unaffected by increasing diffuseness $d_{\bar{v}}$, but the *onset* of convergence (value of N for $S = 1$ or 2) lies at larger values of N.

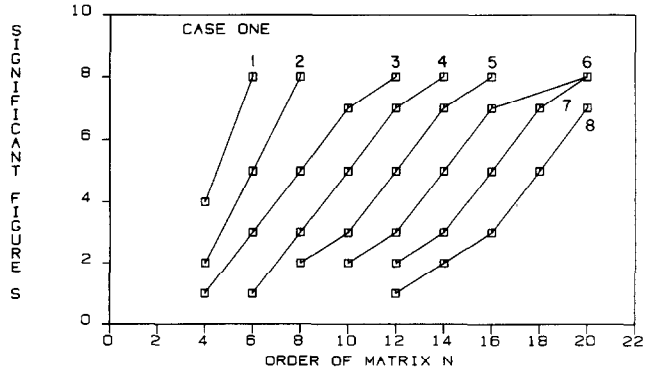

FIG. 1. Rate of convergence to one digit in the Sth decimal as a function of matrix order for the square well with $E = 14.11$ MeV and $l = 0$. The numbers on the curves give the j of the eigenvalue listed as the SQ entry in Table II.

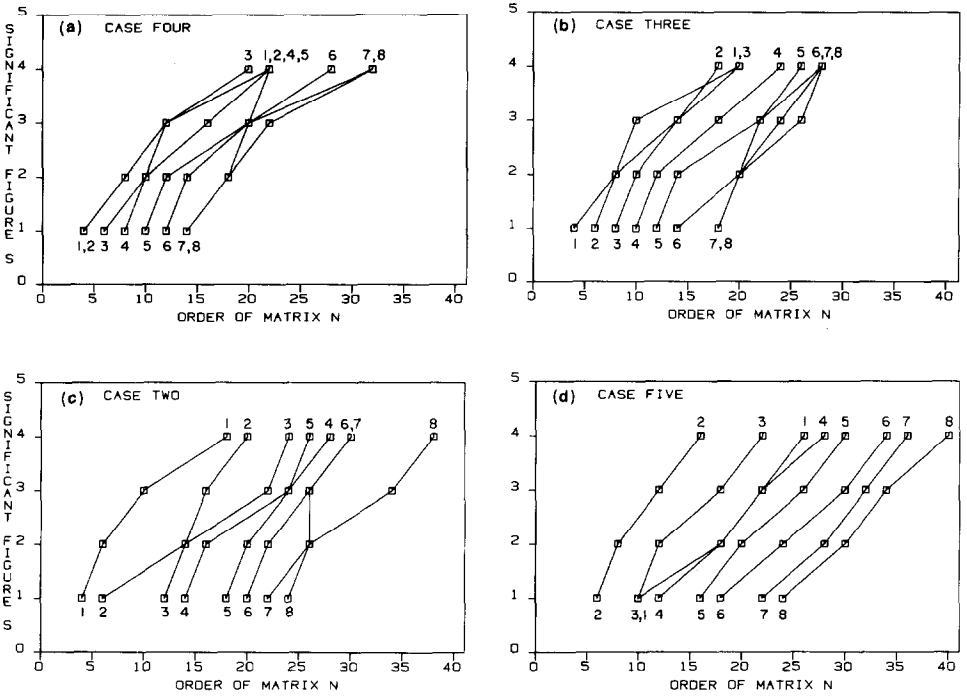

FIG. 2. As in Fig. 1 with (a) case four, (b) case three, (c) case two, (d) case five. The numbers on the curves give the j of the eigenvalue.

D. *Convergence as a Function of Energy E* ($l=0$)

To study how convergence as a function of matrix order N changes as E increases, computations for all five cases were performed in the energy range 14 to 987 MeV. Figure 3 shows $\log(E)$ versus N, where N is the matrix order required to produce the prescribed error of one digit in the fourth significant figure for the first four eigenvalues of cases one to four. There is a moderate trend of increasing N with increasing E for a given eigenvalue. This results largely from the increase in magnitude of a given eigenvalue, for a fixed $\bar{V}(r)$, and as was seen in Table II, larger eigenvalues require a larger N to reach the prescribed error.

E. *Convergence as a Function of l*

The magnitude of all eigenvalues $\lesssim 100$ of case five where $j<10$ and $l<14$ is shown in Fig. 4. This figure shows those eigenvalues which have reached the prescribed error limit as a function of the matrix order N required to achieve this limit. From this figure it is clear that the matrix order required to produce a prerequisite accuracy depends on the absolute magnitude of the eigenvalue. Figure 5 shows a spectral plot of the same eigenvalues ($l<6$) in the complex eigenvalue

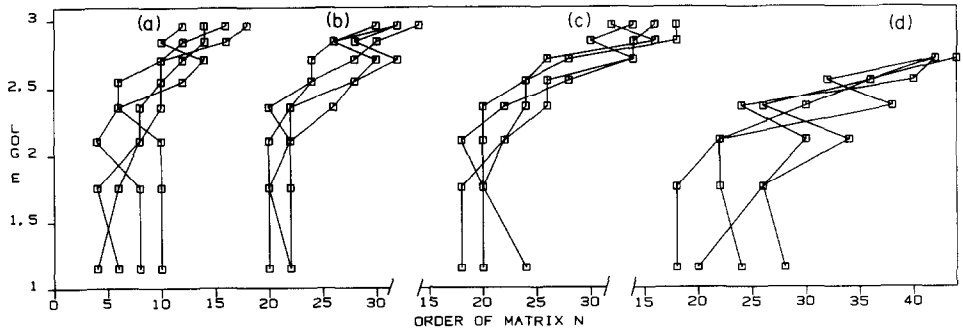

FIG. 3. Convergence as a function of energy (log E) for (a) case one, (b) case four, (c) case three, (d) case two. The points show the order N of the matrix required for convergence of one digit in the fourth figure at each energy for eigenvalues $j=1$ to 4. Different j values are not distinguished as the general trend is similar. Results of case five are similar to those for case two.

plane. From the functional analytic viewpoint the mathematical content of Eq. (3) is displayed in this spectral plot.

Comparison with the marching algorithm results showed good agreement between the two methods, typically within a few digits in the fourth significant figure. The comparison also showed that the marching algorithm fails to find some eigenvalues. Of 127 eigenvalues with $j<10$ and $l<14$ eighteen were not found by the marching algorithm. This is not unexpected since the marching algorithm searches the complex α_{lj} plane and not simply the real line and its degree of success depends on estimates for the location of the α_{lj} in this plane. In contrast to this the R algorithm of rank N always gives N eigenvalues. Furthermore, with increasing N an improved bound on each eigenvalue is obtained until the R algorithm converges to the true eigenvalues of the non-self-adjoint problem of Eq. (3).

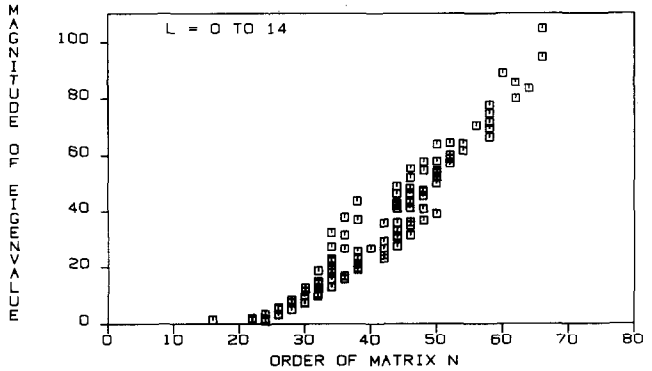

FIG. 4. The matrix order N required to produce convergence of one digit in the fourth figure for $l=0$ to 14, as a function of the magnitude of the eigenvalues for case five. All eigenvalues which have reached this prescribed error are included.

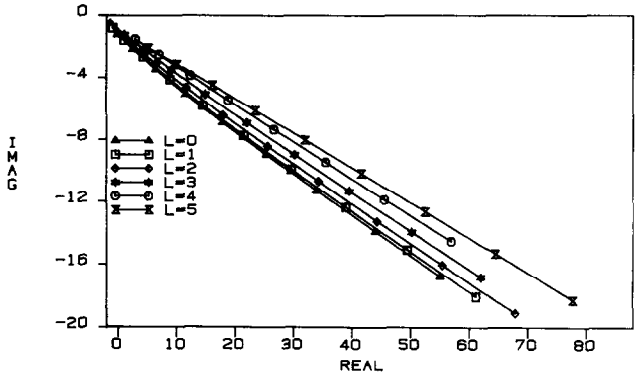

FIG. 5. Spectral plot of eigenvalues for case five in the complex plane for $l=0$ to 5. Only those falling in the ranges chosen for ordinate and abscissa are shown.

VI. CONVERGENCE FOR EIGENFUNCTIONS

Eigenfunctions for the first four eigenvalues of case two ($l=0$) are shown in Fig. 1 of [1]. There it is seen that in general, both real and imaginary parts of eigenfunction v_{lj} have j nodes (including the one at $r=0$) inside the range of the potential $\bar{V}(r)$. Outside the range of $\bar{V}(r)$ all the eigenfunctions v_{lj}, for fixed l, are identical and oscillate with an amplitude unity. These qualitative features already suggest that eigenfunctions for large j require an increasingly higher order polynomial approximation. Furthermore, the approximation is necessary only inside the range of $\bar{V}$.

In this section eigenfunctions of case five only are discussed as this is numerically the most difficult and physically the most realistic example. The eigenfunctions produced by the R algorithm have been compared with those produced by the marching algorithm. Figures 6 and 7 show error curves for $l=0$ and 4, respectively for different j values. In each case the unbroken line is the value of the eigenfunction ϕ_{lj} generated in steps of 0.0078125 fm by the marching algorithm integrating inwards from a marching radius of 11 fm. The results shown are indistinguishable from calculations performed with double this step size. The broken curve shown in the figures is the absolute error

$$A[\phi_{lj}(r)-v_{lj}(r)], \qquad r\in[0,a] \tag{30}$$

where A is a scaling factor and $v_{lj}(r)$ is the eigenfunction, Eq. (7), produced by Algorithm R. All results of Figs. 6 and 7 were obtained from a matrix of order $N_m=66$ but the number of terms N required in Eq. (8) is generally substantially less and varies with l and j. The values of N, l, and j together with real and imaginary parts of the eigenvalues obtained by the R algorithm as well as the magnitude $\sqrt{\alpha_{lj}\alpha_{lj}^*}$ are shown in Figs. 6 and 7. The most accurate results are for

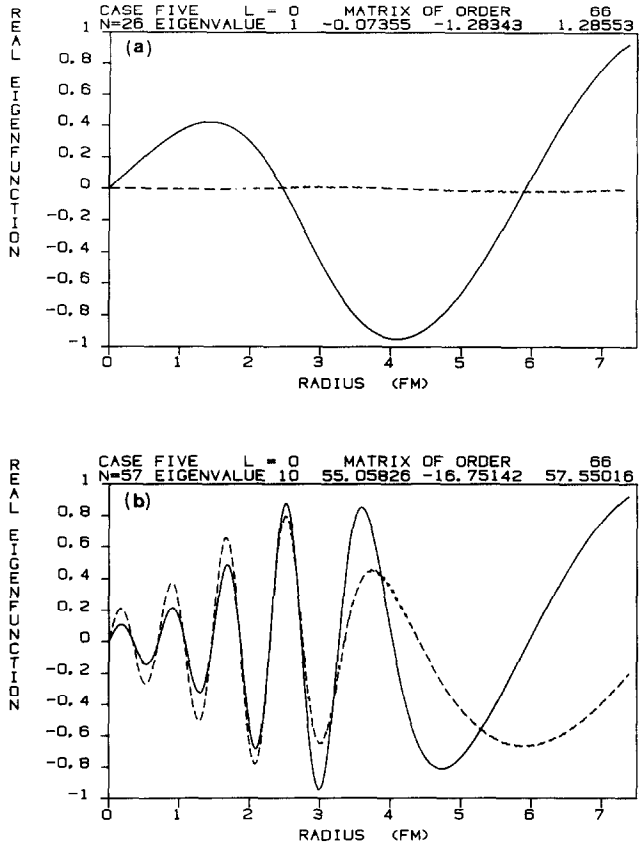

FIG. 6. Eigenfunction for $l=0$ computed by the marching algorithm (unbroken line) and corresponding error curve (dashed line) of Eq. (30) for (a) $j=1$ and (b) $j=10$. The scale factor A of Eq. (30) multiplying the error curve is 100. Only the real part is shown since the results for the imaginary part are similar. Also shown, on the top of each frame, is N the number of terms retained in Eq. (8), the j-value, real and imaginary parts of the eigenvalue, and the magnitude.

$l=0$ where for $j=10$ the absolute error is some two orders of magnitude less than the peaks in the eigenfunction. As l increases the absolute error increases but for $j \gtrsim 2$ and $l<9$ does not become excessive where the eigenfunction has its maximal values inside the potential $\bar{V}$. However, when the eigenfunction is more polynomial-like as for $l=4$, $j=8$ (Fig. 7), the absolute error tends to be substantial at the zeros of the eigenfunction and zero at the maxima. The largest errors occur for $l=8$ (not shown) and in general, as l increases, the eigenfunction inside the interaction region has oscillations of increasing magnitude while outside the interaction region the behaviour is decreasing and monotonic. Thus by $l=14$ (not shown) the amplitude of the oscillations is $\sim 10^5$ and is some three orders of magnitude larger than the eigenfunction in the immediate exterior region.

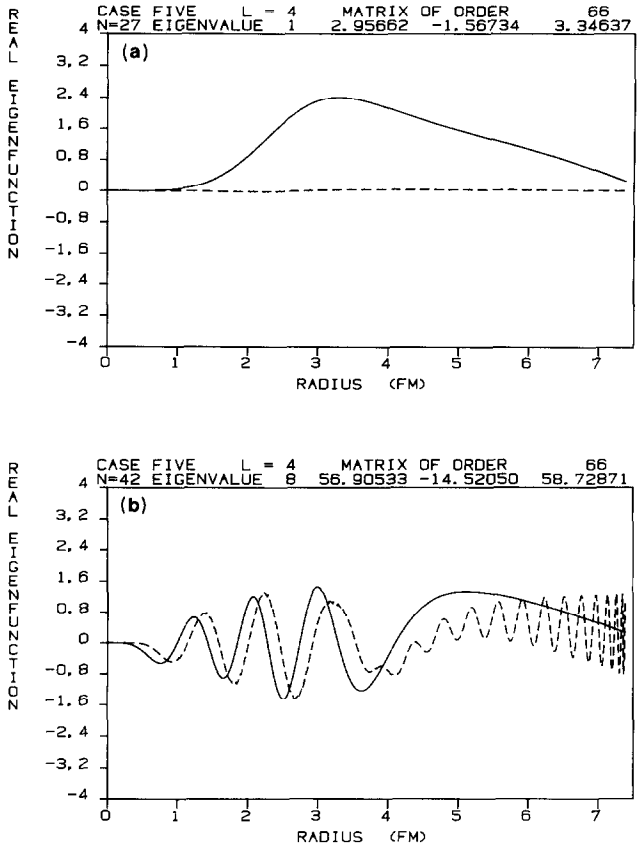

FIG. 7. As in Fig. 6 for $l=4$ and (a) $j=1$, (b) $j=8$. The scale factor A of Eq. (30) multiplying the error curve is 100.

Thus the number of Chebyshev coefficients required to approximate the eigenfunctions for larger l and j increases. Inspection of the eigenfunction confirms that exclusion of the monotonic behaviour in the exterior region from the interval of approximation would improve the approximation on the whole interval $[0, a]$. This is shown in Fig. 8 where the results of case five with $l=6$, $j=7$, are shown for two truncation radii $a=7.39$ and 6.67 fm. With decreasing a the error curve has a reduced amplitude in the exterior region and the approximation on the interval $[0, a]$ improves substantially. This behaviour is typical of all larger j and $l>0$. An empirical criterion for determining the optimal truncation radius a is inspection of the sum, Eq. (8) computed at $r=0$. This sum converges strongly as a is reduced, but will cease to do so when a is reduced beyond an optimal value. Further improvements in the approximation would follow from more accurate computation of the expansion coefficients for the interactions $V_0(r)$, $\bar{V}(r)$, in Eqs. (B1), (B2), or an increase in N_v.

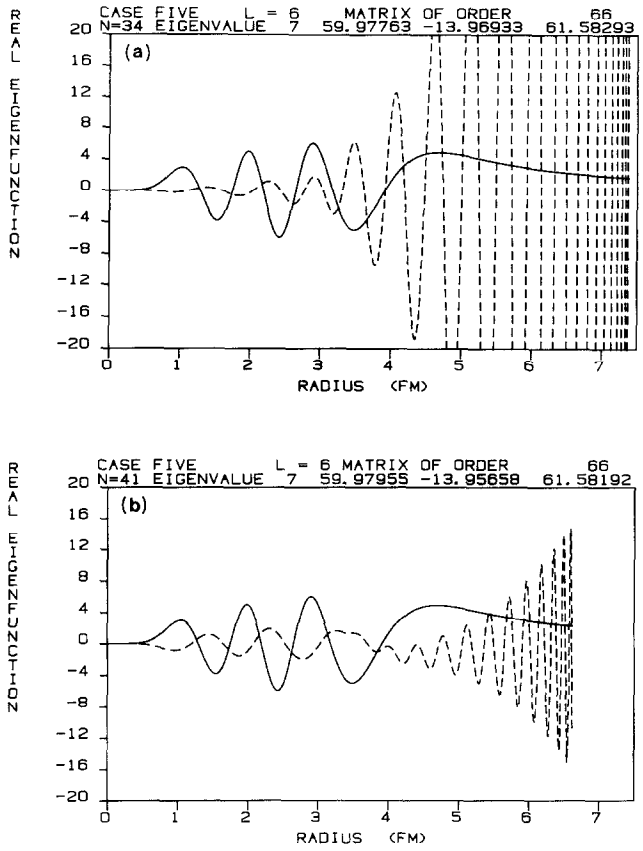

FIG. 8. Eigenfunction for $l = 6$ and $j = 7$ computed by the marching algorithm (unbroken line) and corresponding error curve (dashed line) for the real part with a truncation radius of (a) 7.39 (b) 6.67 fm. Note that the eigenvalue differs slightly as a function of a. The scale factor A of Eq. (30) multiplying the error curve is 10.

However, in physical applications the eigenfunctions need only be well approximated inside the range of $\bar{V}$ since they invariably occur in products with $\bar{V}$ or shorter range interactions and large errors closer to $r = a$ are of less significance.

VII. CONCLUSIONS

The present work proposes the use of a set of linearly independent polynomial approximating functions for solution of Sturmian eigenvalue problems where the linear differential operator is not self-adjoint. Each member of this set satisfies the boundary conditions of the problem and the set is a Chebyshev set. That is, out of the class of approximating polynomials, on the interval of approximation, it

provides a "best" approximation, in the sense of the minimax (or uniform) norm as $N \to \infty$.

In such a truncated basis the Sturmian eigenvalue problem is transformed into a finite, complex general matrix problem which is solved by conventional techniques through application of the R algorithm of Section III. Five case studies confirm that as a function of increasing basis size, the Chebyshev set provides uniform convergence for both eigenvalues and eigenfunctions when compared to the results of a marching algorithm. For a good approximation inside the range of the interaction potentials, the number of basis functions required is not excessive. Furthermore, the number of basis states required is only moderately increased by large variations of physical parameters such as energy E or orbital angular momentum l. The rate of convergence of the method is greatest in the square well case where the interaction is *exactly* reproduced by a finite polynomial approximation. For realistic interaction potentials a good approximation and satisfactory convergence with a moderate number of basis states is still possible with an optimal choice of the truncation radius. This optimal choice depends on the nature of the physical problem, i.e., a knowledge of the fact that for a given energy only a restricted range of orbital angular momenta l are significant and some l values in this range provide the dominant contribution. Thus any approximation scheme should be optimized for those eigenvalues or eigenfunctions which dominate the physical process. A study of the type described here is unable to specify which eigenfunctions are physically more significant and thus need to be well approximated. These and other questions of utility of the basis proposed here are the subjects of study in a problem of physical interest [14] while a comparison of convergence properties of the Chebyshev set with a Bessel function basis is reported elsewhere [6].

The present study has verified the inherent numerical stability of Chebyshev sets for linear non-self-adjoint Sturmian eigenvalue problems. However, improvements in efficiency are still possible and such possibilities as well as a study of mathematical properties of the Hilbert space spanned by the Chebyshev set are subjects under investigation.

APPENDIX A: Boundary Conditions

The boundary conditions on the solutions $v_{lj}(r)$ of Eq. (3) are regular at the origin and "outgoing-waves" asymptotically

$$v_{lj}(r) \underset{r \to 0}{\sim} r^{l+1} \tag{A1}$$

$$v_{lj}(r) \underset{r \to \infty}{\sim} H_l = G_l + iF_l \tag{A2}$$

where $F_l(kr)$ and $G_l(kr)$ are regular and irregular Coulomb functions in the case that U_0 contains a Coulomb term $Z_1 Z_2 e^2/r$. If no Coulomb term is present, then F_l

and G_l are proportional to the radius times j_l and n_l, the spherical Bessel and Neumann functions, respectively.

Continuity of the logarithmic derivative at some point $r = a$ where the potentials U_0 and $\bar{U}$ are negligible requires that

$$\frac{1}{v_{lj}(a)} \frac{dv_{lj}(r)}{dr}\bigg|_{r=a} = \frac{1}{H_l(ka)} \frac{dH_l(kr)}{dr}\bigg|_{r=a} = B_l(ka). \tag{A3}$$

APPENDIX B: CHEBYSHEV COEFFICIENTS FOR U_0, $\bar{U}$, D, AND $\bar{D}$

On the interval $r \in [0, a]$ U_0 and $\bar{U}$ are approximated by Chebyshev polynomials

$$U_0(ax) = \sum_{p=0}^{N_t} \frac{\varepsilon_p}{2} g_p T_{2p}(x) \tag{B1}$$

$$\bar{U}(ax) = \sum_{\bar{p}=0}^{N_t} \frac{\varepsilon_{\bar{p}}}{2} \bar{g}_{\bar{p}} T_{2\bar{p}}(x) \tag{B2}$$

where

$$g_p = \frac{2}{\pi} \int_{-1}^{+1} U_0(|ax|)\, T_{2p}(x) \frac{dx}{\sqrt{1-x^2}} \tag{B3}$$

$$\bar{g}_{\bar{p}} = \frac{2}{\pi} \int_{-1}^{+1} \bar{U}(|ax|)\, T_{2\bar{p}}(x) \frac{dx}{\sqrt{1-x^2}}. \tag{B4}$$

The coefficients in the expansion (26) for the same interval are formally defined by

$$h_m^n = \frac{2}{\pi} \int_{-1}^{+1} a^2 \{k^2 - U_0(|ax|)\}\, t_n^l(x)\, x^2 T_{2m}(x) \frac{dx}{\sqrt{1-x^2}} \tag{B5}$$

$$\bar{h}_{\bar{m}}^n = \frac{2}{\pi} \int_{-1}^{+1} a^2 \bar{U}(|ax|)\, t_n^l(x)\, x^2 T_{2\bar{m}}(x) \frac{dx}{\sqrt{1-x^2}} \tag{B6}$$

or in the notation of Eq. (22)

$$h_m^n = \frac{2}{\pi} a^2 k^2 (t_n^l, x^2 T_{2m}) - \frac{2}{\pi} a^2 (U_0 t_n^l, x^2 T_{2m}) \tag{B7}$$

$$\bar{h}_{\bar{m}}^n = \frac{2}{\pi} a^2 (\bar{U} t_n^l, x^2 T_{2\bar{m}}). \tag{B8}$$

Consider (B8), substituting Eq. (13) for $t_n^l(x)$, applying properties of the Chebyshev polynomials, and substituting

$$\frac{\pi}{2}\bar{g}_{\bar{p}} = (\bar{U}, T_{2\bar{p}})$$

yield

$$\bar{h}_{\bar{m}}^n = \frac{a^2}{8}\{d_n^l(\bar{g}_{\bar{m}+1} + 2\bar{g}_{\bar{m}} + \bar{g}_{|\bar{m}-1|}) + \bar{g}_{n+\bar{m}+1} + 2\bar{g}_{n+\bar{m}} + \bar{g}_{n+|\bar{m}-1|}$$
$$+ \bar{g}_{|n-\bar{m}-1|} + 2\bar{g}_{|n-\bar{m}|} + \bar{g}_{|n-|\bar{m}-1||}\}. \tag{B9}$$

The second term of (B7) is identical to (B9) with $\bar{g}_{\bar{p}}$ replaced by g_p.

If $\bar{U}$ is a square well of radius $R = a$, then from (B4) the only non-zero coefficient $\bar{g}_{\bar{p}}$ is

$$\bar{g}_0 = 2\bar{U} \tag{B10}$$

and (B9) gives the result

$$\bar{h}_0^n = \frac{a^2\bar{U}}{2}\{d_n^l + \delta_{n1}\} \tag{B11}$$

$$\bar{h}_1^n = \frac{a^2\bar{U}}{4}\{d_n^l + 2\delta_{n1} + \delta_{n2}\} \tag{B12}$$

and for $n \geqslant 2$

$$\bar{h}_n^n = \frac{a^2\bar{U}}{2} \tag{B13}$$

$$\bar{h}_n^{n\pm1} = \frac{a^2\bar{U}}{4} \tag{B14}$$

with all other values of $\bar{h}_{\bar{m}}^n$ zero.

The first term on the right-hand side of (B7) is identical to the expressions (B11) to (B14) if $\bar{U}$ is replaced by k^2.

APPENDIX C: Evaluation of the Normalization Integral

With the expansion of Eq. (12) for $u_{ij}(r)$ and another of the form (B2) for $\bar{V}(r)$, both for the same interval $r \in [0, a]$, the integral of Eq. (29) may be evaluated by recurrence on applying properties of Chebyshev polynomials. The product of two Chebyshev series may be written as a third Chebyshev series (see Sect. 8.6.1 of Luke

[8]). Defining such a product in the integrand of (29), the integral which remains, namely,

$$I_n^{l+1} = \int_0^1 dx\, x^{2l+2} T_{2n}(x) \tag{C1}$$

is generated by recurrence as follows. If N and L are the maximum values of n and l respectively, then

$$I_n^0 = -1/(4n^2-1), \qquad n = 0,..., N+L+1, \tag{C2}$$

$$4I_n^{l+1} = I_{n+1}^l + 2I_n^l + I_{|n-1|}^l, \qquad l = 0,..., L,\ n = N+L,..., 1, \tag{C3}$$

and

$$I_0^{l+1} = 1/(2l+3). \tag{C4}$$

Checking the recurrence (C3) against the analytical result (C4) for $l=0$ to 50 and $n=0$ to 80 reveals an order of accuracy better than 10^{-15} when working to sixteen decimals.

ACKNOWLEDGMENTS

The authors are grateful for use of computing facilities at the Universities of Connecticut and Witwatersrand. This work was begun during G. Delic's study leave at the University of Connecticut during the winter of 1981–1982. This visit was made possible by grants from the U.S. Department of Energy (Contract DE-AC-02-77-ER 04444-A004), the Council for Scientific and Industrial Research (R.S.A.), and the University of Connecticut Research Foundation. This support is gratefully acknowledged. G. Delic also wishes to express his appreciation to Professor Rawitscher for his kind hospitality and for the stimulating collaboration.

REFERENCES

1. G. H. RAWITSCHER, *Phys. Rev. C* **25** (1982), 2196.
2. W. T. REID, "Sturmian Theory for Ordinary Differential Equations," Springer-Verlag, New York, 1980.
3. T. J. RIVLIN, "The Chebyshev Polynomials," Wiley–Interscience, New York, 1974.
4. L. V. KANTOROVICH AND G. P. AKILOV, "Functional Analysis," 2nd ed., Pergamon Press, New York, 1982.
5. H. M. NUSSENZVEIG, *Nucl. Phys.* **11** (1959), 499.
6. G. H. RAWITSCHER AND G. DELIC, Sturmian eigenvalue equations on a bessel function basis, submitted for publication.
7. G. DELIC, *Comput. Phys. Commun.* **18** (1979), 73.
8. Y. L. LUKE, "The Special Functions and Their Approximation," Vol. I, Academic Press, New York, 1969.
9. J. R. RICE, "The Approximation of Functions," Vol. I, Addison–Wesley, Reading, Mass., 1964.
10. G. DELIC, "Formulae for Numerical Differentiation and Integration," IKDA 73/8, June 1973.

11. C. BARDIN, Y. DANDEU, L. GAUTHIER, J. GUILLEMIN, T. LENA, J.-M. PERNET, H. H. WOLTER, AND T. TAMURA, *Comput. Phys. Commun.* **3** (1972), 73.
12. B. T. SMITH, J. M. BOYLE, J. J. DONGARRA, B. S. GARBOW, Y. IKEBE, V. C. KLEMA, AND C. B. MOLER, "Matrix Eigensystem Routines – EISPACK Guide," 2nd ed., Springer-Verlag, New York, 1976.
13. G. DELIC AND G. H. RAWITSCHER, *Bull. Amer. Phys. Soc.* **27** (1982), 576.
14. G. H. RAWITSCHER AND G. DELIC, *Phys. Rev. C* **29** (1984), 747 and 1153.